⌘ *Author's Choice*

Activation of 5-HT$_{2A/C}$ Receptors Counteracts 5-HT$_{1A}$ Regulation of *N*-Methyl-D-aspartate Receptor Channels in Pyramidal Neurons of Prefrontal Cortex*

Eunice Y. Yuen, Qian Jiang, Paul Chen, Jian Feng, and Zhen Yan[1]

From the Department of Physiology and Biophysics, School of Medicine and Biomedical Sciences, State University of New York, Buffalo, New York 14214

Abnormal serotonin-glutamate interaction in prefrontal cortex (PFC) is implicated in the pathophysiology of many mental disorders, including schizophrenia and depression. However, the mechanisms by which this interaction occurs remain unclear. Our previous study has shown that activation of 5-HT$_{1A}$ receptors inhibits *N*-methyl-D-aspartate (NMDA) receptor (NMDAR) currents in PFC pyramidal neurons by disrupting microtubule-based transport of NMDARs. Here we found that activation of 5-HT$_{2A/C}$ receptors significantly attenuated the effect of 5-HT$_{1A}$ on NMDAR currents and microtubule depolymerization. The counteractive effect of 5-HT$_{2A/C}$ on 5-HT$_{1A}$ regulation of synaptic NMDAR response was also observed in PFC pyramidal neurons from intact animals treated with various 5-HT-related drugs. Moreover, 5-HT$_{2A/C}$ stimulation triggered the activation of extracellular signal-regulated kinase (ERK) in dendritic processes. Inhibition of the β-arrestin/Src/dynamin signaling blocked 5-HT$_{2A/C}$ activation of ERK and the counteractive effect of 5-HT$_{2A/C}$ on 5-HT$_{1A}$ regulation of NMDAR currents. Immunocytochemical studies showed that 5-HT$_{2A/C}$ treatment blocked the inhibitory effect of 5-HT$_{1A}$ on surface NR2B clusters on dendrites, which was prevented by cellular knockdown of β-arrestins. Taken together, our study suggests that serotonin, via 5-HT$_{1A}$ and 5-HT$_{2A/C}$ receptor activation, regulates NMDAR functions in PFC neurons in a counteractive manner. 5-HT$_{2A/C}$, by activating ERK via the β-arrestin-dependent pathway, opposes the 5-HT$_{1A}$ disruption of microtubule stability and NMDAR transport. These findings provide a framework for understanding the complex interactions between serotonin and NMDARs in PFC, which could be important for cognitive and emotional control in which both systems are highly involved.

Serotonin (5-HT)[2] is a key neuromodulator mediating diverse cognitive and emotional functions in the central nervous system (1). The pleiotropic functions of serotonin are afforded by the concerted actions of multiple 5-HT receptor subtypes, 5-HT$_1$- to 5-HT$_7$ (2, 3). Mice lacking 5-HT receptors exhibit phenotypes ranging from increased anxiety (4), to elevated aggression (5), to antidepressant-like behaviors (6). One of the major targets of serotonin is prefrontal cortex (PFC), a crucial brain region controlling emotion and cognition (7, 8). Several lines of evidence have shown that 5-HT$_{1A}$ and 5-HT$_{2A}$ receptors, which are abundantly co-expressed in most of PFC pyramidal neurons (9), often have opposing actions on common substrates. For instance, activation of 5-HT$_{1A}$ receptors results in neuronal inhibition by increasing potassium currents (10) and decreasing calcium currents (11). In contrast, 5-HT$_{2A}$ receptor stimulation leads to neuronal excitation by suppressing potassium currents (2) and enhancing pre-synaptic glutamate release (12). Moreover, elevated 5-HT$_{1A}$ receptors and reduced 5-HT$_{2A}$ receptors are found in PFC of schizophrenia patients (13, 14), suggesting that the levels of 5-HT$_{1A}$ and 5-HT$_{2A}$ receptors are differentially altered in diseased states.

One of the potential cellular targets of 5-HT receptors involved in cognitive and emotional control is the NMDA-type glutamate receptor, a ligand-gated ion channel that has been implicated in the pathophysiology of mental disorders (15). NMDAR hypofunction caused by systemic administration of non-competitive NMDAR antagonists or knockdown of NMDAR expression produces schizophrenia-like behavioral symptoms (16–18). Moreover, it has been found that the expression of NMDARs is reduced in postmortem brains of depressed patients (19), and chronic antidepressant treatment enhances NMDAR levels in mouse brains (20). Our previous study has shown that activation of 5-HT$_{1A}$ receptors suppresses NMDAR channel function in PFC pyramidal neurons (21). It remains unknown whether 5-HT$_{2A}$ receptor activation has any impact on the 5-HT$_{1A}$-NMDAR interaction.

[1] To whom correspondence should be addressed: Dept. of Physiology and Biophysics, School of Medicine and Biomedical Sciences, State University of New York, 124 Sherman Hall, Buffalo, NY 14214. Tel.: 716-829-3058; Fax: 716-829-2699; E-mail: zhenyan@buffalo.edu.

[2] The abbreviations used are: 5-HT, serotonin; NMDA, *N*-methyl-D-aspartate; NMDAR, NMDA receptor; MAP, microtubule-associated protein; MAP2, microtubule-associated protein 2; PFC, prefrontal cortex; ERK, extracellular signal-regulated kinase; ANOVA, analysis of variance; GABA$_A$, γ-aminobutyric acid, type A; 8-OH-DPAT, 8-hydroxy-2(di-*n*-propylamino)-tetralin; PP2, 4-amino-5-(4-chlorophenyl)-7-(*t*-butyl)pyrazolo[3,4-*d*]pyrimidine; PP3, 4-amino-7-phenylpyrazol[3,4-*d*]pyrimidine; siRNA, small interference RNA; GFP, green fluorescent protein; MES, 4-morpholineethanesulfonic acid; fluox, fluoxetine; ket, ketanserin; α-Me-5HT, α-methyl-5-hydroxytryptamine maleate; EPSC, excitatory postsynaptic current.

Here we show that activation of 5-HT$_{1A}$ and 5-HT$_{2A/C}$ receptors in PFC pyramidal neurons regulates NMDAR channels in a counteractive manner by converging on the microtubule-based transport of NMDARs that is regulated by ERK. Given the importance of NMDAR and serotonin in mental processes under normal and pathological conditions, the complex regulation of NMDAR function by 5-HT$_{1A}$ and 5-HT$_{2A/C}$ receptors may provide a molecular and cellular mechanism underlying the role of serotonin in regulating cognitive and emotional behaviors.

EXPERIMENTAL PROCEDURES

Whole Cell Recordings—Whole cell current recordings of cultured PFC neurons employed standard voltage-clamp techniques as those we described previously (21, 22). The external solution for recording NMDAR-mediated current contained (in mM): 127 NaCl, 20 CsCl, 1 CaCl$_2$, 10 HEPES, 5 BaCl$_2$, 12 glucose, 0.001 tetrodotoxin, and glycine 0.02, pH 7.3–7.4, 300–305 mosM/liter. The internal solution contained (in mM): 180 N-methyl-D-glucamine, 4 MgCl$_2$, 40 HEPES, 0.5 1,2-bis(2-aminophenoxy)ethane-N,N,N',N'-tetraacetic acid, 12 phosphocreatine, 3 Na$_2$ATP, and 0.5 Na$_2$GTP, 0.1 leupeptin, pH 7.2-3, 265–270 mosM/liter. Recordings were obtained with an Axon Instruments (Union City, CA) 200B patch clamp amplifier that was monitored by an IBM PC running pClamp 8 with a DigiData 1320 series interface. Electrode resistances were normally 2–4 MΩ in bath solution. Following seal rupture, series resistance (4–10 MΩ) was compensated (70–90%). Attention was applied to monitor the series resistance, and recordings were stopped when a significant increase (>20%) occurred. The whole cell NMDAR-mediated current was evoked by NMDA (100 μM) application for 2 s every 30 s with neurons held at −60 mV. Drugs were applied with a "sewer pipe" system. The array of drug capillaries was positioned a few hundred micrometers from the cell under recording. Solution changes were controlled by the SF-77B fast-step solution stimulus delivery device (Warner Instruments, Hamden, CT). Data were analyzed with AxoGraph (Axon instruments) and KaleidaGraph (Albeck Software). ANOVA was performed to compare the differential degrees of current regulation between experimental groups subjected to different drug treatment. Data are expressed as the mean ± S.E.

Electrophysiological Recordings in Slices—To record NMDAR-mediated synaptic transmission, we performed the standard whole cell recording techniques in layer V PFC pyramidal neurons (21, 23). Patch pipettes (5–9 MΩ) were filled with the following internal solution (in mM): 130 cesium methanesulfonate, 10 CsCl, 4 NaCl, 1 MgCl$_2$, 10 HEPES, 5 EGTA, 2.2 QX-314, 12 phosphocreatine, 5 MgATP, 0.5 Na$_2$GTP, 0.1 leupeptin, pH 7.2–7.3, 265–270 mosM/liter. PFC slices (300 μm) were perfused at room temperature (22–24 °C), with artificial cerebrospinal fluid was bubbled with 95% O$_2$/5% CO$_2$ containing 6-cyano-7-nitroquinoxaline-2,3-dione (20 μM) and bicuculline (10 μM) to block α-amino-3-hydroxy-5-methyl-4-isoxazoleproprionic acid/kainite receptors and GABA$_A$ receptors, respectively. Neurons were observed with a 40× water-immersion lens and illuminated with near infrared IR light, and the image was captured with an IR-sensitive charge-coupled device camera. All recordings were performed using a Multiclamp 700A amplifier. Upon application of negative pressure, the membrane was tightly sealed with resistance (2–10 GΩ). With additional suction, the membrane was disrupted into the whole cell configuration. The access resistances ranged from 13 to 18 MΩ with 50–70% compensation. Evoked currents were generated with a pulse from a stimulation isolation unit controlled by an S48 pulse generator (Astro-Med). A bipolar stimulating electrode (Fredrick Haer Company) was positioned ~100 μm from the neuron upon recording. Prior to stimulation, neurons (clamped at −70 mV) were depolarized to +60 mV for 3 s to fully eliminate the voltage-dependent Mg^{2+} block of NMDAR. Age-matched saline controls were done side-by-side with drug-injected animals on each day of experiments. To minimize variations between slices, the stimulus with the same intensity was delivered by the stimulating electrode placed at the same location. Data analyses were performed with the Clampfit software (Axon Instruments).

The agents we used include serotonin, 8-hydroxy-2(di-n-propylamino)tetralin (8-OH-DPAT), α-Me-5HT, (−)-2,5-dimethoxy-4-iodoamphetamine, ketanserin, benzothiazole, colchicine (Sigma), dynamin inhibitory peptide (Tocris), 4-amino-5-(4-chlorophenyl)-7-(t-butyl)pyrazolo[3,4-d]pyrimidine (PP2) and 4-amino-7-phenylpyrazol[3,4-d]pyrimidine (PP3) (Calbiochem). They were made up as concentrated stocks in water or DMSO and stored at −20 °C. Stocks were thawed and diluted immediately prior to experiments.

Animal Treatment—Young male rats (25–28 days old) were administered intraperitoneally with the drugs as described in the text. For stereotaxic injection, rats were anesthetized with pentobarbital sodium (50 mg/kg intraperitoneal) and then mounted into a stereotaxic apparatus (David Kopf Instruments). Fluoxetine (fluox) (2 μl, 0.34 mg/ml, dissolved in saline) were injected unilaterally into the PFC region using a Hamilton syringe (22-gauge needle) at a rate of 0.5 μl/min. The coordinates of the lateral PFC used are 1.0–1.4 mm lateral from midline, 2.2 mm anterior to Bregma, and 3.3 mm dorsal to ventral.

Small Interfering RNA—To knock down the endogenous β-arrestin expression, we used the small interfering RNA (siRNA) that specifically targets β-arrestin1 or β-arrestin2 mRNA (24). The siRNA oligonucleotide sequences were: 5′-GGCGAGUCUACGUGACACUtt-3′ (for β-arrestin1) and 5′-GGACCGGAASGUGUUUGUGtt-3′ (for β-arrestin2). The siRNA (purchased from Ambion, Austin, TX) was co-transfected with enhanced GFP into cultured PFC neurons (11 days *in vitro*) using the Lipofectamine 2000 method. Biochemical, immunocytochemical, or electrophysiological experiments were performed in neurons after 2–3 days of transfection.

Measurement of Free Tubulin—Free tubulin from PFC cultures was extracted as described previously (21). Cultured PFC neurons (2 × 10^5 cells/cm^2, 14 days *in vitro*) in 3.5-cm dishes were washed twice at 37 °C with 1 ml of microtubule stabilizing buffer containing (0.1 M MES (pH 6.75), 1 mM MgSO$_4$, 2 mM EGTA, 0.1 mM EDTA, and 4 M glycerol). Cultures were then incubated at 37 °C for 5 min in 600 μl of soluble tubulin extraction buffer (0.1 M MES (pH 6.75), 1 mM MgSO$_4$, 2 mM EGTA, 0.1 mM EDTA, 4 M glycerol, and 0.1% Triton X-100) with the addition of protease inhibitor mixture tablets (Roche Applied Science). The soluble extract was centrifuged at 37 °C for 2 min, and the supernatant was collected. Equal amounts of total pro-
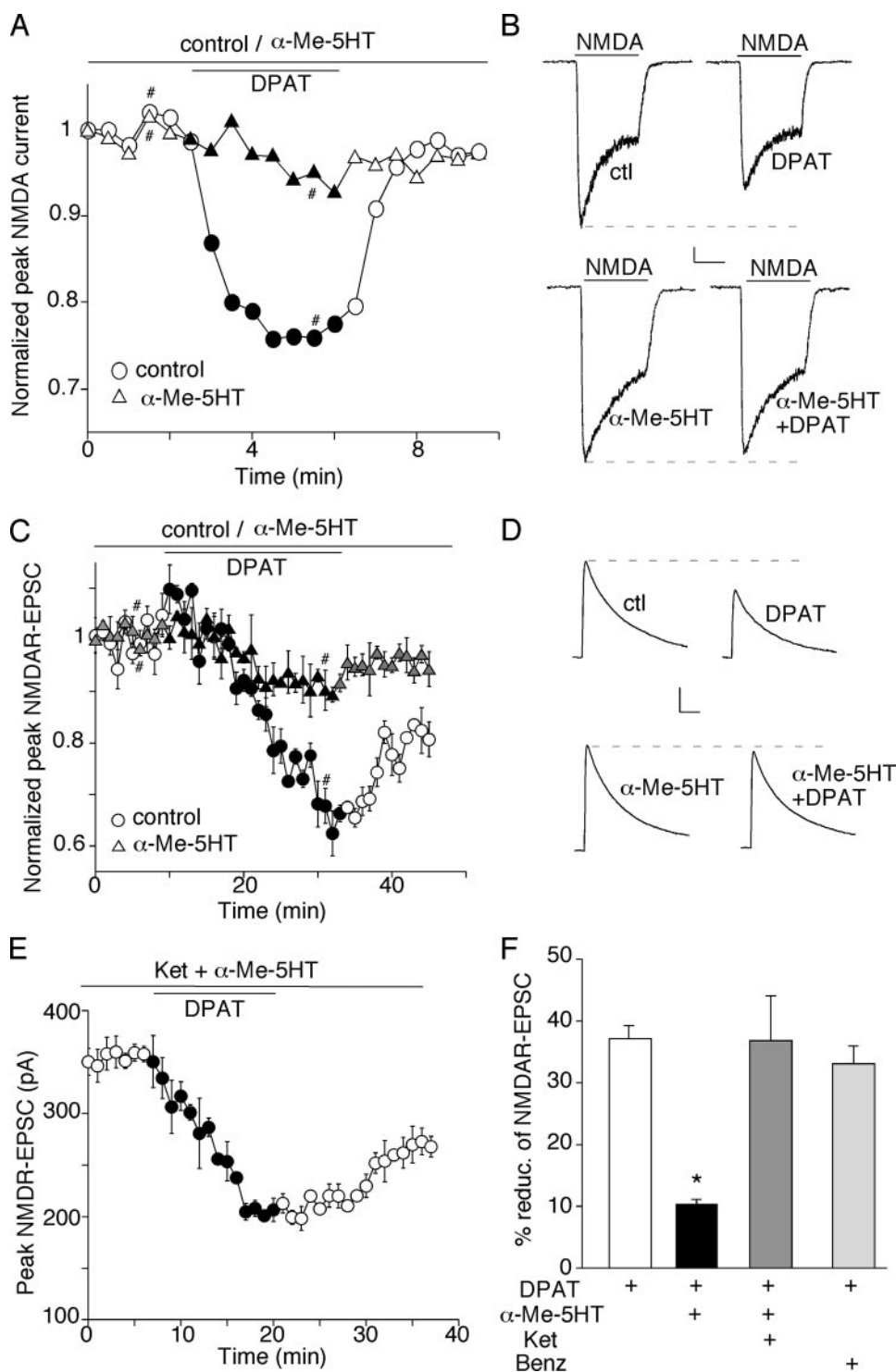
FIGURE 1. **Activation of 5-HT$_{2A/C}$ receptors counteracts the 5-HT$_{1A}$-induced reduction of NMDAR-mediated ionic and synaptic currents in PFC pyramidal neurons.** *A* and *C*, plot of normalized peak NMDAR currents (*A*) or NMDAR-EPSC (*C*) as a function of time and 8-OH-DPAT (5-HT$_{1A}$ agonist, 20 μM) application in neurons treated with or without α-Me-5HT (5-HT$_{2A/C}$ agonist, 20 μM). Each point (*C*) represents the average peak (mean ± S.E.) of three consecutive NMDAR-EPSC. *B* and *D*, representative current traces taken from the records used to construct *A* or *C* (at time points denoted by #). *Scale bars*: 100 pA, 1 s (*B*); 100 pA, 100 ms (*D*). *E*, plot of peak NMDAR-EPSC showing the effect of 8-OH-DPAT (20 μM) in the presence of α-Me-5HT (20 μM) and ketanserin (5-HT$_{2A/C}$ antagonist, 20 μM). *F*, cumulative data (mean ± S.E.) summarizing the percentage reduction of NMDAR-EPSC by 8-OH-DPAT in the presence or absence of various 5-HT receptor agonists or antagonists. *, $p < 0.001$, ANOVA.

Immunocytochemical Staining— The detection of surface GFP-NR2B (25) was performed as how we described before (21, 22). Briefly, cultured PFC neurons were treated with various agents after transfection, and then fixed in 4% paraformaldehyde for 30 min at room temperature without permeabilization. After incubating in 5% bovine serum albumin to block nonspecific staining, cells were incubated with the anti-GFP antibody (1:100, Chemicon, Temecula, CA) for 1 h at room temperature. After three washes in phosphate-buffered saline, cells were incubated with a rhodamine-conjugated secondary antibody (1: 200, Sigma) for 1 h at room temperature. After washing in phosphate-buffered saline, coverslips were mounted on slides with Vectashield mounting media (Vector Laboratories, Burlingame, CA). Fluorescence images were detected using a 60× objective with a cooled charge-coupled device camera mounted on a Nikon microscope.

The surface GFP-NR2B clusters were analyzed with ImageJ software. All specimens were imaged under identical conditions and analyzed with identical parameters. A 50-μm segment of dendrite was selected from the equal distance away from the soma of four to six individual neurons. To define dendritic clusters, a single threshold was selected manually. Signal was counted as clusters when its intensity was 2- to 3-fold greater than the overall fluorescence on the dendritic shaft. Three to four independent experiments were performed. Quantitative analyses were performed blindly without knowledge of experimental conditions.

Biochemical Measurement of Surface Receptors—After treatment, PFC slices were incubated with artificial cerebrospinal fluid containing 1 mg/ml Sulfo-NHS-LC-Biotin (Pierce) for 20 min on ice. The slices were then rinsed three times in Tris-buffered saline to quench the biotin reaction, followed by homogenization in 300 μl of modified radioimmune precipitation assay buffer (1% Triton X-100, 0.1% SDS, 0.5% deoxycholic acid, 50 mM NaPO$_4$, 150 mM NaCl, 2 mM

tein were analyzed by Western blotting using anti-α-tubulin (Sigma). The intensity of tubulin bands was quantitatively analyzed with Image (National Institutes of Health).

EDTA, 50 mM NaF, 10 mM sodium pyrophosphate, 1 mM sodium orthovanadate, 1 mM phenylmethylsulfonyl fluoride, and 1 mg/ml leupeptin). The homogenates were centrifuged at $14,000 \times g$ for 15 min at 4 °C. 15 μg of homogenates was removed to measure total proteins. For surface protein detection, 150 μg of homogenates was incubated with 100 μl of 50% NeutrAvidin-Agarose (Pierce) for 2 h at 4 °C, and bound proteins were resuspended in 25 μl of SDS sample buffer and boiled. Quantitative Western blots were performed on both total and biotinylated (surface) proteins using anti-NR1, anti-NR2B (Upstate Biotechnology, Lake Placid, NY), and anti-GABA$_A$R β2/3 (Chemicon).

RESULTS

Activation of 5-HT$_{1A}$ and 5-HT$_{2A/C}$ Receptors Regulates NMDAR-mediated Ionic and Synaptic Currents in a Counteractive Manner—We have previously found that activation of 5-HT$_{1A}$ receptors reduces NMDAR currents in PFC pyramidal neurons (21). To examine the potential interactions between 5-HT$_{1A}$ and 5-HT$_{2A/C}$ receptors on NMDAR functions, we tested the impact of 5-HT$_2$ activation on 5-HT$_{1A}$ regulation of NMDAR currents by preincubating PFC cultures with the 5-HT$_{2A/C}$ agonist α-Me-5HT (20 μM, 10–30 min). Application of NMDA (100 μM) elicited an inward current that was partially desensitized and was completely eliminated by the NMDA receptor antagonist D-aminophosphonovalerate (50 μM). As shown in Fig. 1 (*A* and *B*), application of the 5-HT$_{1A}$ agonist 8-OH-DPAT (20 μM) reversibly reduced NMDAR currents ($21.3 \pm 0.7\%$, $n = 16$). However, in α-Me-5HT-treated neurons, the reduction of NMDAR current by 8-OH-DPAT was substantially attenuated ($6.4 \pm 0.7\%$, $n = 8$). α-Me-5HT alone did not significantly affect NMDAR currents (1 μM: $4.0 \pm 0.8\%$, $n = 5$; 20 μM: $5.7 \pm 1.4\%$, $n = 7$). Another 5-HT$_{2A/C}$ agonist DOI also had no effect on NMDAR currents at low doses (0.05 μM: $4.2 \pm 1.2\%$, $n = 5$; 0.1 μM: $4.0 \pm 2.5\%$, $n = 5$), which are different from the inhibitory effect of DOI shown before (26). The discrepancy may be due to different experimental procedures in recording NMDA-induced currents. In a previous study (26), microdrops of NMDA (1 mM, every 15 min) were applied to PFC slices, which did not allow the accurate detection of peak NMDA currents because of the slow diffusion of the ligand. Moreover, it was not a pure postsynaptic preparation like dissociated neurons, which could have indirect effects due to changes in the circuit. Our results suggest that 5-HT$_{2A/C}$ activation alone does not directly affect NMDAR currents but opposes 5-HT$_{1A}$ regulation of NMDAR currents in PFC pyramidal neurons.

We further tested the influence of 5-HT$_2$ activation on 5-HT$_{1A}$ regulation of NMDAR-EPSC mediated by synaptic NMDA receptors in PFC slices. As shown in Fig. 1 (*C* and *D*), application of 8-OH-DPAT potently reduced the amplitude of NMDAR-EPSC ($37.1 \pm 2.1\%$; $n = 10$ (Fig. 1*F*)). However, this reduction was significantly attenuated in the presence of α-Me-5HT ($10.4 \pm 0.7\%$; $n = 13$ (Fig. 1*F*)). To verify that 5-HT$_{2A/C}$ receptors were mediating this regulatory effect of α-Me-5HT, we pre-treated PFC slices with the specific 5-HT$_{2A/C}$ antagonist ketanserin (20 μM). As shown in Fig. 1*E*, α-Me-5HT failed to oppose the effect of 5-HT$_{1A}$ on NMDAR-EPSC in the presence of ketanserin ($36.8 \pm 7.1\%$; $n = 5$ (Fig. 1*F*)). In contrast, the reduction of NMDAR-EPSC by 8-OH-DPAT was intact in the
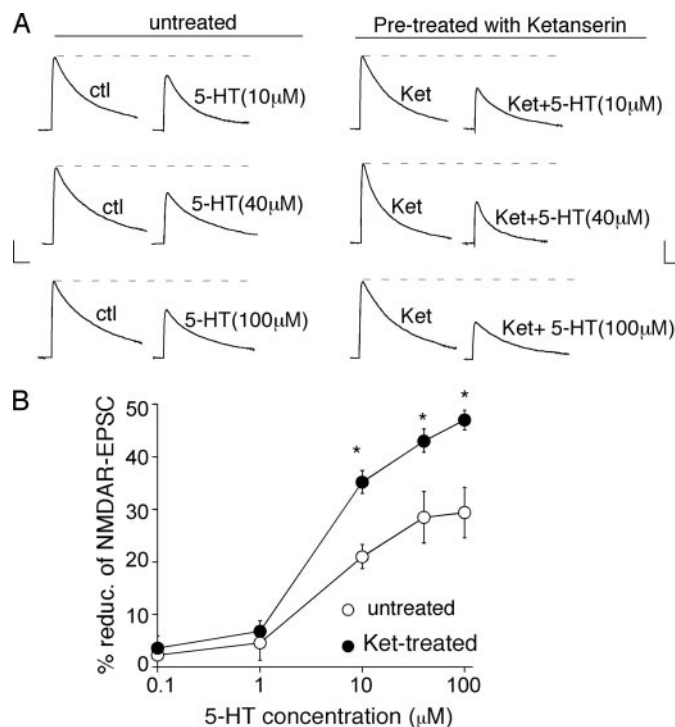

FIGURE 2. Inhibition of 5-HT$_{2A/C}$ receptors unmasks the 5-HT$_{1A}$-mediated reduction of NMDAR-EPSC in response to 5-HT. *A*, representative NMDAR-EPSC traces (average of three trials) showing the regulation of NMDAR-EPSC by 5-HT (10, 40, or 100 μM) in neurons treated with or without the 5-HT$_{2A/C}$ antagonist ketanserin (*ket*, 20 μM). *Scale bars*: 100 pA, 100 ms. *B*, dose-response curves summarizing the percentage reduction of NMDAR-EPSC by different concentrations of 5-HT in neurons treated with or without ketanserin. *, $p < 0.001$, ANOVA.

presence of the 5-HT$_4$ agonist benzothiazole (20 μM, $33 \pm 2.9\%$; $n = 5$ (Fig. 1*F*)). These results indicate that 5-HT$_{2A/C}$ receptor activation selectively counteracts 5-HT$_{1A}$ regulation of NMDAR functions in PFC pyramidal neurons.

We next examined what would happen when both 5-HT$_{1A}$ and 5-HT$_{2A/C}$ receptors are co-activated by serotonin. If both signals oppose each other, then blocking one receptor activation would unmask the effect of the other. Thus, we tested the effect of serotonin on NMDAR-EPSC in PFC slices treated with or without 5-HT$_2$ antagonists. As shown in Fig. 2 (*A* and *B*), different concentrations of serotonin reduced the amplitude of NMDAR-EPSC to different extents (10 μM: $21 \pm 2.3\%$, $n = 4$; 40 μM: $28.5 \pm 4.9\%$, $n = 4$; 100 μM: $29.4 \pm 4.8\%$, $n = 5$). However, in the presence of the 5-HT$_{2A/C}$ antagonist ketanserin (20 μM), the reduction of NMDAR-EPSC by serotonin was greatly augmented (10 μM: $35.2 \pm 2.2\%$, $n = 7$; 40 μM: $43.0 \pm 2.0\%$, $n = 6$; 100 μM: $47 \pm 1.9\%$, $n = 7$). It suggests that 5-HT$_2$ receptor activation in response to serotonin masks part of the inhibitory action of 5-HT$_{1A}$ receptors on NMDAR channels.

To assess whether the serotonergic regulation of NMDARs, which we found *in vitro*, is also occurring *in vivo*, we tested whether endogenous serotonin, via the activation of 5-HT$_{1A}$ and 5-HT$_{2A/C}$ receptors, could regulate NMDAR functions in a similar manner in intact animals. First, we examined NMDAR-EPSC in PFC slices from animals intraperitoneally injected with 5-HT$_{1A}$ or 5-HT$_{2A/C}$ agonists. As shown in Fig. 3*A*, the amplitude of NMDAR-EPSC was significantly smaller in animals intraperitoneally injected with the 5-HT$_{1A}$ agonist 8-OH-
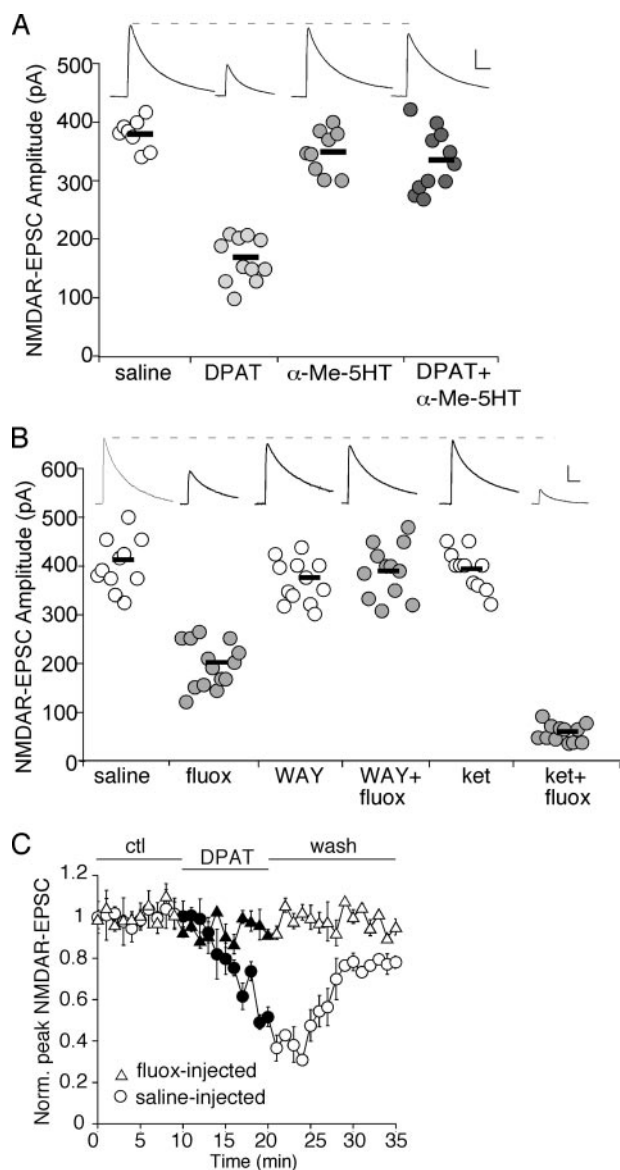
FIGURE 3. **The synaptic NMDA response is reduced in PFC pyramidal neurons from animals with systemic administration of 5-HT$_{1A}$ agonist or the serotonin re-uptake inhibitor fluoxetine, which is opposed by injecting 5-HT$_{2A/C}$ agonist.** *A* and *B*, dot plots showing the peak amplitude of NMDAR-EPSC recorded in PFC pyramidal neurons from animals with a single intraperitoneal injection of different drugs. *A*, saline, 8-OH-DPAT, α-Me-5HT, or 8-OH-DPAT plus α-Me-5HT; *B*, saline, fluoxetine, WAY-100635, WAY-100635 plus fluoxetine, ketanserin, or ketanserin plus fluoxetine. All drugs were at the concentration of 20 mg/kg. Animals were sacrificed for slicing 1 h after drug administration. Mean values of each group are indicated by *short bars*. *Inset*: representative NMDAR-EPSC traces recorded in PFC pyramidal neurons from animals with different drug injection. *Scale bars*: 100 pA, 100 ms. *C*, plot of normalized peak NMDAR-EPSC showing the effect of bath application of 8-OH-DPAT (40 μM) in PFC pyramidal neurons from animals intraperitoneally injected with fluoxetine (20 mg/kg) or saline.

DPAT (saline: 379.8 ± 8.9 pA, *n* = 8; DPAT: 166 ± 11.5 pA, *n* = 11; *p* < 0.001, ANOVA), whereas it was largely unaltered by injecting the 5-HT$_{2A/C}$ agonist α-Me-5HT (349 ± 12.2 pA, *n* = 10). However, the effect of 8-OH-DPAT injection was blocked by injecting α-Me-5HT (DPAT + α-Me-5HT: 335 ± 15.9 pA, *n* = 12). These results indicate that activation of 5-HT$_{1A}$ receptors *in vivo* down-regulates NMDAR functions, and this effect of 5-HT$_{1A}$ is opposed by 5-HT$_{2A/C}$ receptor activation *in vivo*.
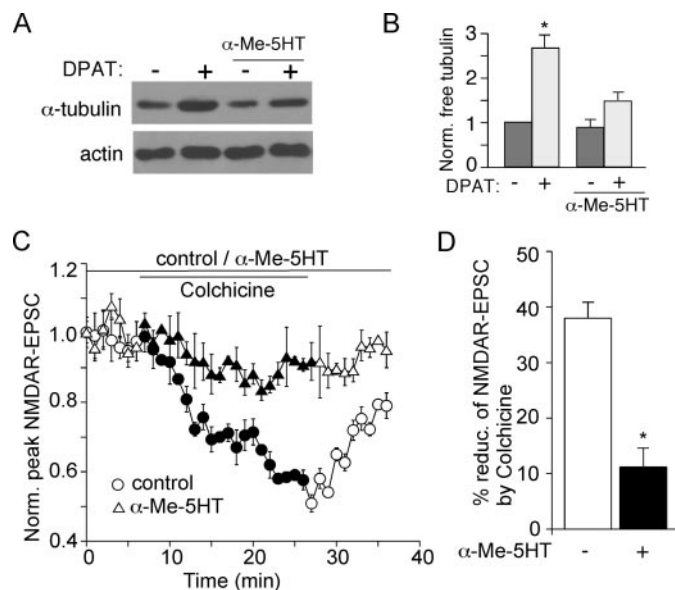
FIGURE 4. **Activation of 5-HT$_{2A/C}$ receptors attenuates the 5-HT$_{1A}$ -induced microtubule depolymerization and the effect of microtubule depolymerizer on NMDAR-EPSC.** *A*, Western blot analysis of free tubulin in lysates of cultured PFC neurons treated with or without 8-OH-DPAT (40 μM, 30 min) in the absence or presence of α-Me-5HT (20 μM, added 10 min before 8-OH-DPAT treatment). *B*, quantification of free tubulin assay. Free tubulin level was normalized to control ($-$), based on the intensity of the tubulin band from Western blot analyses. Each *point* represents mean ± S.E. of 4–5 independent experiments. *, *p* < 0.001, ANOVA. *C*, plot of normalized peak NMDAR-EPSC showing the effect of microtubule depolymerizer colchicine (30 μM) in the absence or presence of α-Me-5HT (20 μM). *D*, cumulative data (mean ± S.E.) illustrating the percent reduction of NMDAR-EPSC by colchicine in neurons with or without the exposure to α-Me-5HT. *, *p* < 0.05, ANOVA.

Moreover, the amplitude of α-amino-3-hydroxy-5-methyl-4-isoxazoleproprionic acid receptor-EPSC was unchanged by 8-OH-DPAT injection (saline: 113 ± 11.8 pA, *n* = 11; DPAT: 112 ± 9.9 pA, *n* = 10), suggesting that 5-HT$_{1A}$ activation in PFC is specifically targeting postsynaptic NMDARs rather than presynaptic glutamate release.

Next, we examined NMDAR-EPSC in PFC slices from animals intraperitoneally injected with the serotonin re-uptake inhibitor fluoxetine (20 mg/kg) to elevate endogenous 5-HT levels at synapses. As shown in Fig. 3*B*, the amplitude of NMDAR-EPSC in fluoxetine-injected animals was significantly smaller, compared with saline controls (saline: 403.5 ± 15.8 pA, *n* = 11; fluox: 195.1 ± 12.4 pA, *n* = 14; *p* < 0.001, ANOVA). This effect of fluoxetine was blocked by injecting the 5-HT$_{1A}$ antagonist WAY-100635 (WAY: 367 ± 12.9 pA, *n* = 12; WAY + fluox: 390 ± 15.8 pA, *n* = 12), suggesting the mediation by 5-HT$_{1A}$ receptors. Moreover, the reducing effect of fluoxetine on NMDAR-EPSC was potentiated by injecting the 5-HT$_{2A/C}$ antagonist ketanserin (ket: 392 ± 12.3 pA, *n* = 11; ket + fluox: 59.6 ± 5.2 pA, *n* = 12; *p* < 0.001, ANOVA), revealing the counteracting effect of 5-HT$_{2A/C}$ on 5-HT$_{1A}$ regulation of synaptic NMDA responses. Moreover, the effect of bath application of 8-OH-DPAT (40 μM) on NMDAR-EPSC was occluded in animals injected with fluoxetine, as compared with saline controls (Fig. 3*C*, saline: 40.2 ± 1.9%, *n* = 5, fluox: 10.5 ± 2.5%, *n* = 6), confirming the common mechanism underlying the *in vivo* fluoxetine effect and *in vitro* 8-OH-DPAT effect on NMDARs. In contrast to the strong effect in PFC pyramidal
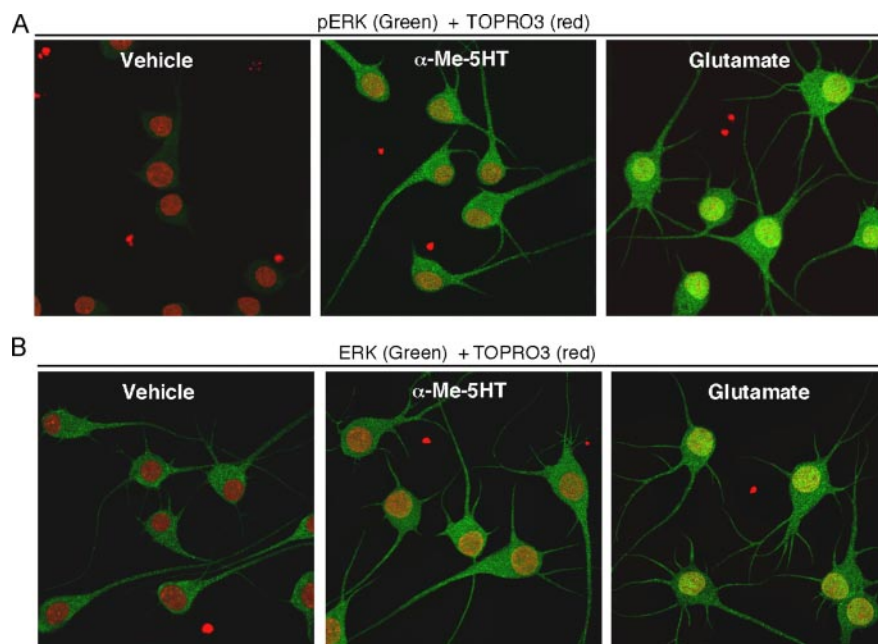
FIGURE 5. **Activation of 5-HT$_{2A/C}$ receptors induces the phosphorylation and activation of ERK in neuronal dendrites in cultured PFC neurons.** *A* and *B*, immunocytochemical images of cultured PFC neurons stained with phospho-ERK (*A*, *green*) or ERK (*B*, *green*) plus the nucleus marker TOPRO3 (*red*) in the absence (vehicle) or presence of α-Me-5HT (20 μM, 3 min) or glutamate (100 μM, 3 min).
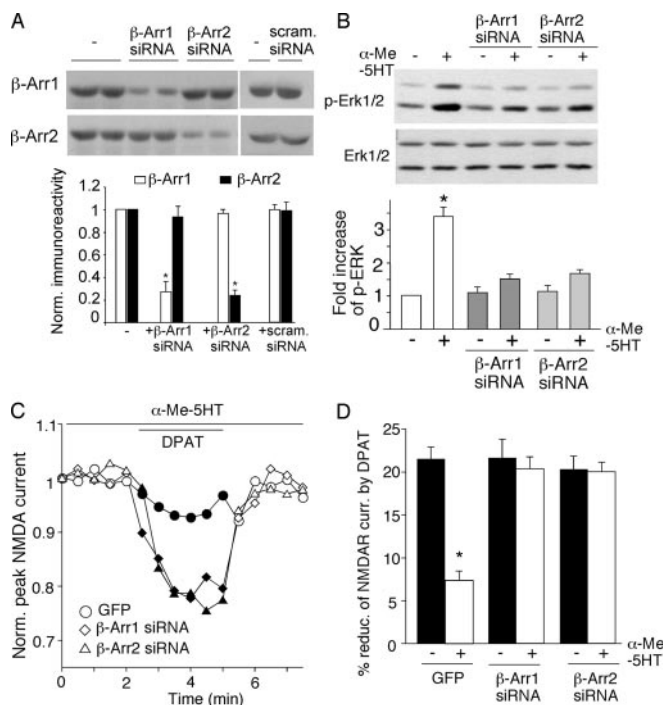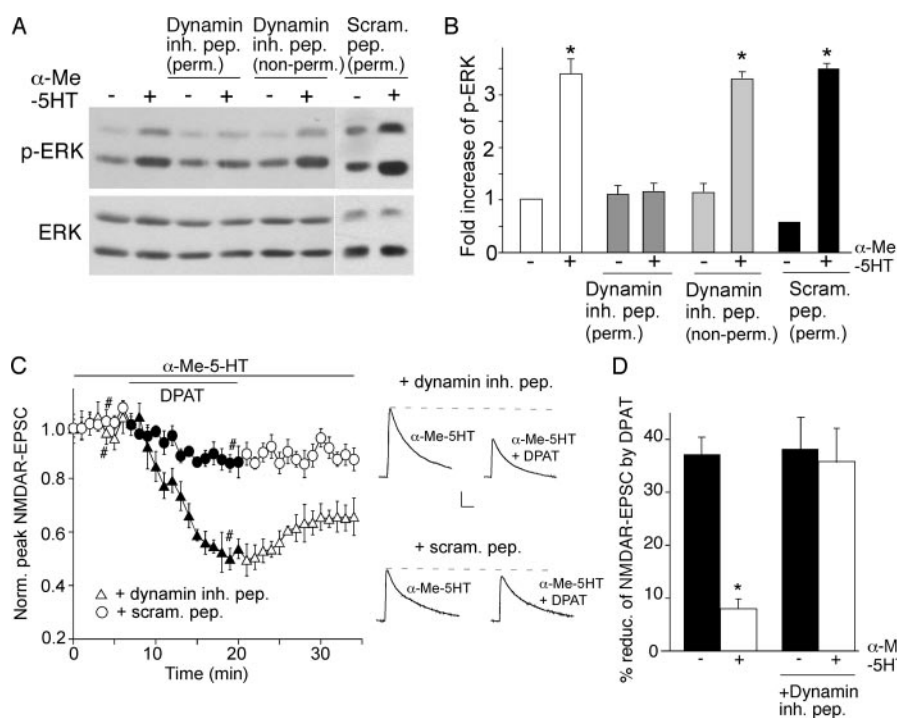

FIGURE 6. **The counteractive effect of 5-HT$_{2A/C}$ on 5-HT$_{1A}$ regulation of NMDAR function is dependent on the β-arrestin/ERK pathway.** *A, top*: Western blots of β-arrestin 1/2 in PFC cultures transfected without or with siRNA against β-arrestin 1/2 or a scrambled siRNA. Quantification of β-arrestin 1/2 expression under different conditions. Each *point* represents mean ± S.E. of three independent experiments. *, $p < 0.001$, ANOVA. *B, top*: Western blots of phospho-ERK in the absence or presence of α-Me-5HT (20 μM, 3 min) in PFC cultures transfected with or without β-arrestin 1/2 siRNA. *Bottom*: quantification of phospho-ERK under different conditions. Each *point* represents mean ± S.E. of 4–5 independent experiments. *, $p < 0.001$, ANOVA. *C*, plot of peak NMDAR currents as a function of time and 8-OH-DPAT (20 μM) application in the presence of α-Me-5HT (20 μM) in GFP-positive neurons transfected with or without siRNA against β-arrestin 1/2. *D*, cumulative data (mean ± S.E.) summarizing the percentage reduction of NMDAR currents by 8-OH-DPAT in the absence or presence of α-Me-5HT under different conditions. *, $p < 0.001$, ANOVA.

neurons, fluoxetine injection failed to affect NMDAR-EPSC in striatal medium spiny neurons (saline: 375 ± 15.9 pA, $n = 8$; fluox: 351 ± 13.9 pA, $n = 10$), suggesting the specificity of serotonergic regulation of NMDARs in PFC.

To further test the effect of 5-HT on NMDARs in PFC networks *in vivo* without affecting other circuits, we also performed stereotaxic injection of fluoxetine to PFC to elevate the local 5-HT levels. We found that the amplitude of NMDAR-EPSC in PFC pyramidal neurons localized at the proximity of injection sites was significantly smaller, compared with saline controls (saline: 401 ± 10.1 pA, $n = 11$; fluox: 162 ± 13.2 pA, $n = 11$, $p < 0.001$, ANOVA).

The Opposing Regulation of NMDA Receptors by 5-HT$_{1A}$ and 5-HT$_2$ Receptors Depends on Microtubule Stability—Next, we investigated the potential mechanism by which 5-HT$_2$ receptors counteract the effect of 5-HT$_{1A}$ on NMDAR currents in PFC neurons. Previously, we have found that 5-HT$_{1A}$ disrupts NMDA receptor trafficking by destabilizing microtubule integrity (21). Thus, we examined whether microtubule dynamics is the convergent target of 5-HT$_{1A}$- and 5-HT$_{2A}$-mediated signaling. To test this, we compared the level of free (depolymerized) tubulin in PFC cultures subjected to 8-OH-DPAT treatment in the absence or presence of α-Me-5HT. As shown in Fig. 4 (*A* and *B*), application of 8-OH-DPAT (40 μM, 20 min) caused a potent increase in free tubulin (1.7 ± 0.3-fold increase, $n = 3$, $p < 0.001$, ANOVA), however, this effect was significantly blocked by α-Me-5HT (20 μM, 0.6 ± 0.2-fold increase, $n = 3$), indicating that 5-HT$_2$ activation could increase microtubule stability and prevent 5-HT$_{1A}$-induced microtubule depolymerization.

We then tested whether the counteractive effect of 5-HT$_2$ on 5-HT$_{1A}$ regulation of NMDAR currents is due to the opposing regulation of microtubule dynamics by 5-HT$_{1A}$ and 5-HT$_2$ receptors. As shown in Fig. 4 (*C* and *D*), bath application of the microtubule depolymerizer, colchicine (30 μM), gradually reduced NMDAR-EPSC in PFC slices (38.0 ± 2.9%, $n = 5$, also see Ref. 22), mimicking and occluding the 5-HT$_{1A}$ effect (21). However, this inhibitory effect of colchicine was largely attenuated in the presence of α-Me-5HT (20 μM, 11.2 ± 13.4%, $n = 6$). These results suggest that activation of 5-HT$_{1A}$ and 5-HT$_2$ receptors could regulate NMDAR currents in a counteractive manner by converging on microtubule dynamics.

Activation of 5-HT$_2$ Receptors Induces ERK Activation in Neuronal Processes—How could 5-HT$_2$ activation increase microtubule stability? Evidence has shown that activation of ERK stabilizes microtubule integrity (27, 28). Moreover, our previous findings have suggested that 5-HT$_{1A}$ reduces ERK activity, which in turn reduces MAP2 phosphorylation and

FIGURE 7. **The counteractive effect of 5-HT$_{2A/C}$ on 5-HT$_{1A}$ regulation of NMDAR function involves clathrin/dynamin-mediated endocytosis.** *A,* Western blots of phospho-ERK and total ERK in PFC cultures treated with or without α-Me-5HT (20 μM, 3 min) in the absence or presence of the cell-permeable (myristoylated) or non-permeable dynamin inhibitory peptide (both 50 μM), or a cell-permeable scrambled control peptide (50 μM). This scrambled peptide was fused with the protein transduction domain of the human immunodeficiency virus TAT protein (YGRKKRRQRRR, 53), which rendered it cell-permeable. All peptides were added 30 min before α-Me-5HT treatment. *B,* quantification of phospho-ERK under different conditions. Each *point* represents mean $\pm$ S.E. of 4–5 independent experiments. *, $p < 0.001$, ANOVA. *C,* plot of normalized peak NMDAR-EPSC showing the effect of 8-OH-DPAT (20 μM) in the presence of α-Me-5HT (20 μM) in cells dialyzed with the dynamin inhibitory peptide (50 μM) or a scrambled control peptide (50 μM). *Inset,* representative traces of NMDAR-EPSC taken at time points denoted by #. *Scale bars*: 100 pA, 10 ms. *D,* cumulative data (mean $\pm$ S.E.) summarizing the percentage reduction of NMDAR-EPSC by 8-OH-DPAT in the absence or presence of α-Me-5HT in neurons injected with or without the dynamin inhibitory peptide. *, $p < 0.001$, ANOVA.

microtubule stability (21). Thus, we speculate that 5-HT$_2$ receptors might activate ERK, leading to increased phosphorylation of MAP2 and its association with microtubules. To test this, we measured the activation of ERK1/2 in response to 5-HT$_{2A/C}$ agonists with an antibody that recognizes activated EKR1/2, which are doubly phosphorylated at Thr-202/Tyr-204 in the activation loop of the kinases (29). As a positive control, we also treated neurons with glutamate, which was reported to activate ERK (30). As shown in Fig. 5*A*, application of α-Me-5HT (20 μM, 3 min) or glutamate (100 μM, 3 min) increased ERK phosphorylation, as compared with vehicle-treated neurons. Unlike glutamate treatment, the α-Me-5HT-activated ERK did not co-localize with TOPRO3 (a nucleus marker) staining, suggesting that 5-HT$_2$-activated ERK is mainly targeted to the cytoplasm rather than nucleus. Among all experimental groups, total ERK levels remained unchanged (Fig. 5*B*). These data suggest that 5-HT$_2$ receptors induce ERK activation, which may oppose the down-regulation of ERK by 5-HT$_{1A}$ receptors.

The β-Arrestin-mediated Pathway Is Involved in the Counteractive Effects of 5-HT$_2$ Receptors on 5-HT$_{1A}$ Regulation of NMDAR Currents—Next, we sought to identify the signaling mechanism underlying 5-HT$_2$ activation of ERK. Recently, it has been shown that some G proteins form a signaling complex with the multifunctional adaptor and transducer molecule, β-ar-

restins 1/2, which recruits and activates components of the mitogen-activated protein kinase cascades (31, 32). To examine the possibility that 5-HT$_2$ receptors activate ERK through the β-arrestin pathway, we transfected PFC cultures with siRNA against β-arrestin1 or -2 to knock down their expression. As shown in Fig. 6*A*, the protein level of β-arrestin1 or -2 was selectively reduced by β-arrestin1 siRNA or β-arrestin2 siRNA, respectively, but not by a scrambled siRNA. The α-Me-5HT-induced activation of ERK1/2 was markedly blocked by knockdown of β-arrestin1 or -2 (Fig. 6*B*). The total ERK level was not affected among all experimental conditions. It suggests that 5-HT$_2$ receptors activate ERK through a mechanism depending on β-arrestins.

β-Arrestin is highly expressed in postsynaptic synapses of glutamatergic neurons (33), where both 5-HT receptors and NMDA receptors are abundant. To test whether 5-HT$_2$ activation of ERK is required for the counteracting effect of 5-HT$_2$ on 5-HT$_{1A}$ modulation of NMDAR channels, we examined the effect of 8-OH-DPAT on NMDAR currents in the presence of α-Me-5HT in PFC cultures trans-

fected with siRNA against β-arrestin1 or -2. No significant differences in NMDAR current densities were found in neurons with different transfections (GFP: 20.1 $\pm$ 1.3 pA/picofarad, $n = 11$; β-arrestin1 siRNA: 20 $\pm$ 1.2 pA/picofarad, $n = 7$; β-arrestin2 siRNA: 19.5 $\pm$ 0.8 pA/picofarad, $n = 11$). In addition, the effect of 8-OH-DPAT on NMDAR currents was the same in all experimental groups. However, α-Me-5HT failed to counteract the 8-OH-DPAT reduction of NMDAR currents in GFP-positive neurons transfected with β-arrestin1 or β-arrestin2 siRNA (Fig. 6*C*: β-arrestin1 siRNA: 20.3 $\pm$ 1.4%, $n = 7$; Fig. 6*D*: β-arrestin2 siRNA: 20.0 $\pm$ 1.1%, $n = 11$), as compared with neurons transfected with GFP alone (7.4 $\pm$ 1.2%; $n = 11$). Taken together, these data suggest that β-arrestins are involved in the counteractive effect of 5-HT$_2$ on 5-HT$_{1A}$ regulation of NMDAR currents in PFC neurons.

Because dynamin-dependent endocytosis of G protein-coupled receptor is required for G protein-coupled receptor/β-arrestin-induced ERK signaling (34), we further examined the role of dynamin in the counteractive effect of 5-HT$_2$ on 5-HT$_{1A}$ regulation of NMDAR currents. PFC cultures were treated with a dynamin inhibitory peptide, which competes for binding to amphiphysin and hence inhibits the clathrin/dynamin-dependent endocytosis (35). As shown in Fig. 7 (*A* and *B*), treatment of PFC cultures with the membrane-permeable dynamin inhibi-
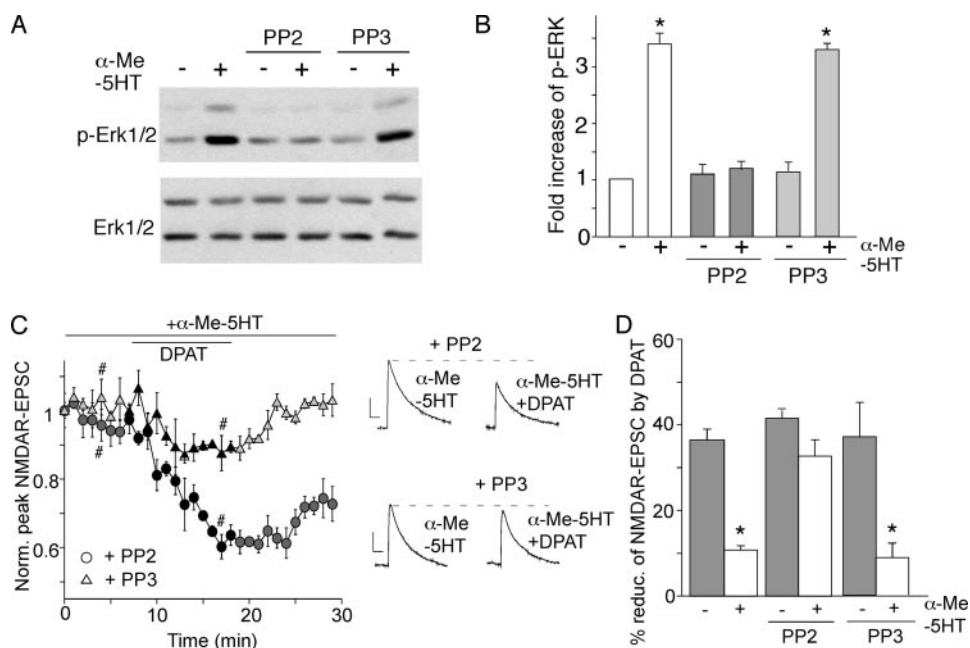
FIGURE 8. Inhibition of Src prevents 5-HT$_{2A/C}$ from opposing 5-HT$_{1A}$ regulation of NMDAR currents. *A*, Western blots of phospho-ERK and total ERK in PFC cultures treated with or without α-Me-5HT (20 μM, 3 min) in the absence or presence of the Src kinase inhibitor PP2 or its inactive homolog PP3 (both 10 μM, added 30 min before α-Me-5HT treatment). *B*, quantification of phospho-ERK under different conditions. Each *point* represents mean $\pm$ S.E. of 4–5 independent experiments. *, $p < 0.001$, ANOVA. *C*, plot of normalized peak NMDAR-EPSC showing the effect of 8-OH-DPAT (20 μM) in the presence of α-Me-5HT (20 μM) in cells injected with PP2 (20 μM) or PP3 (20 μM). *Inset*, representative traces of NMDAR-EPSC (average of three trials) taken at time points denoted by #. *Scale bars*: 100 pA, 100 ms. *D*, cumulative data (mean $\pm$ S.E.) showing the percent reduction of NMDAR-EPSC by 8-OH-DPAT in the absence or presence of α-Me-5HT under different conditions. *, $p < 0.001$, ANOVA.

NMDAR trafficking on microtubules in an opposite way. To test this, we performed immunocytochemical experiments in cultured PFC neurons transfected with GFP-tagged NR2B subunits (the GFP tag is positioned at the extracellular N terminus of NR2B). Surface NR2B receptors were detected with the anti-GFP primary antibody, followed by rhodamine-conjugated secondary antibody in non-permeabilized conditions. Consistent with our previous findings (21), application of 8-OH-DPAT (40 μM, 5 min), caused a marked reduction in the number and size of surface NR2B clusters (Fig. 9, *A* and *B*), as compared with control neurons (cluster density: 43.6 $\pm$ 1.7 clusters/50 μm in controls *versus* 22.7 $\pm$ 0.8 clusters/50 μm in DPAT-treated cells; cluster size: 0.33 $\pm$ 0.02 μm^2 in controls *versus* 0.18 $\pm$ 0.02 μm^2 in DPAT-treated cells (Fig. 9*G*). Treatment with α-Me-5HT (40 μM, 30 min) significantly prevented the 8-OH-DPAT-induced reduction of surface NR2B subunits (cluster density: 40.0 $\pm$ 2.7 clusters/50 μm; cluster size: 0.3 $\pm$ 0.03 μm^2 (Fig. 9, *C* and *G*)). The α-Me-5HT treatment itself did not affect the distribution of surface NR2B clusters (data not shown). The fluorescence intensity of surface NR2B clusters (average gray value per pixel) was not significantly changed in neurons subject to various treatments (Fig. 9*G*). The total amount of recombinant NR2B receptor (GFP channel) was unaltered.

Next, we examined the signaling molecules involved in 5-HT$_2$ blockade of 5-HT$_{1A}$ reduction of surface NR2B clusters. To test this, we co-transfected PFC cultures with β-arrestin2 siRNA and GFP-tagged NR2B subunits. As shown in Fig. 9 (*D* and *E*), transfection of β-arrestin2 alone did not affect the distribution of surface NR2B clusters (cluster density: 38.1 $\pm$ 3.1 clusters/50 μm; cluster size: 0.29 $\pm$ 0.01 μm^2 (Fig. 9*G*)) or the reducing effect of 8-OH-DPAT on NR2B clusters (cluster density: 22.8 $\pm$ 0.8 clusters/50 μm; cluster size: 0.16 $\pm$ 0.03 μm^2 (Fig. 9*G*)). However, knockdown of β-arrestin2 prevented α-Me-5HT from blocking the 8-OH-DPAT-induced reduction of surface NR2B clusters on dendrites (cluster density: 23.4 $\pm$ 1.6 clusters/50 μm; cluster size: 0.17 $\pm$ 0.02 μm^2 (Fig. 9, *F* and *G*)). These results suggest that activation of 5-HT$_2$ receptors opposes 5-HT$_{1A}$ reduction of the surface NR2B level through a β-arrestin-dependent mechanism.

Finally, we tested whether the change on NMDAR-EPSC amplitudes in PFC neurons by acute fluoxetine treatment of intact animals can be accounted for by the altered number of NMDA receptors on the cell membrane. Surface biotinylation experiments (23) were performed to measure levels of surface NR1 and NR2B in PFC slices from animals intraperitoneally

tory peptide (50 μM) markedly blocked the α-Me-5HT-induced ERK activation, whereas the membrane-impermeable dynamin inhibitory peptide or a cell-permeable scrambled control peptide was ineffective. Furthermore, in neurons injected with the dynamin inhibitory peptide (50 μM), α-Me-5HT failed to counteract the 5-HT$_{1A}$ reduction of NMDAR-EPSC (35.8 $\pm$ 6.3%, $n = 5$ (Fig. 7, *C* and *D*)). Together, these data suggest that dynamin-based 5-HT$_2$ receptor endocytosis is involved in 5-HT$_2$ activation of ERK and 5-HT$_2$ opposing of 5-HT$_{1A}$ regulation of NMDAR currents.

Previous studies have suggested that Src-mediated tyrosine phosphorylation of dynamin is involved in G protein-coupled receptor-induced ERK signaling (31, 36). To test whether Src kinase activity is required for 5-HT$_2$ activation of ERK and the counteractive effect of 5-HT$_2$ on 5-HT$_{1A}$ regulation of NMDAR currents, we measured the effect of α-Me-5HT in PFC neurons treated with the Src kinase inhibitor, PP2. As shown in Fig. 8 (*A* and *B*), application of PP2 (20 μM), but not the inactive analog PP3 (20 μM), significantly blocked the α-Me-5HT-induced ERK phosphorylation. The total ERK level was not affected in cells subjected to different treatments. Moreover, in the presence of PP2, but not PP3, α-Me-5HT lost the ability to oppose 8-OH-DPAT reduction of NMDAR-EPSC (Fig. 8*C*: PP2: 32.7 $\pm$ 3.7%, $n = 7$; Fig. 8*D*: PP3: 8.8 $\pm$ 3.3%, $n = 4$). Taken together, these results suggest that Src kinase activation is involved in 5-HT$_2$ signaling.
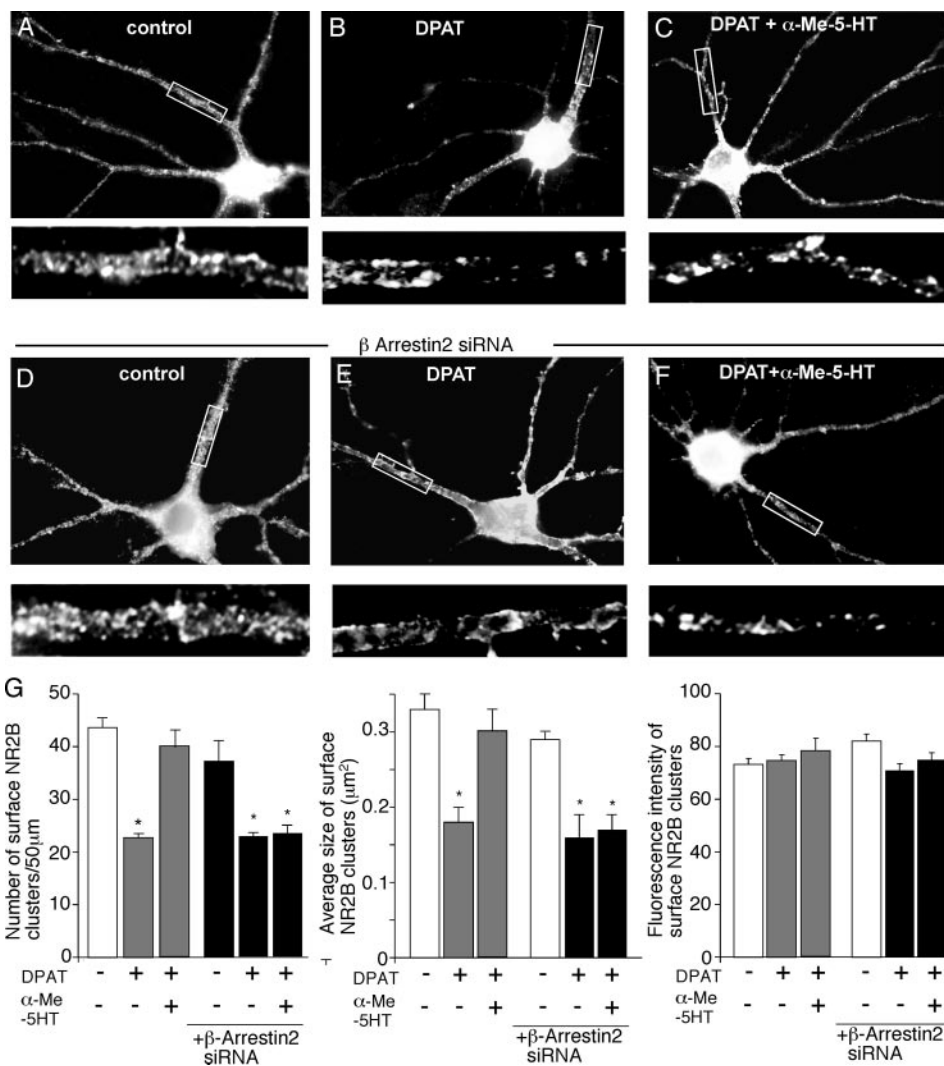
Activation of 5-HT$_2$ Receptors Opposes 5-HT$_{1A}$ Reduction of Surface NR2B Subunits in a β-Arrestin-dependent Manner—If 5-HT$_{1A}$ and 5-HT$_{2A/C}$ regulate microtubule dynamics in a counteractive manner, it is possible that they may alter

FIGURE 9. **Activation of 5-HT$_{2A/C}$ receptors opposes the 5-HT$_{1A}$ -induced decrease of surface NR2B clusters on neuronal dendrites.** *A–F*, immunocytochemical images of surface GFP-NR2B clusters in PFC cultures transfected with or without β-arrestin2 siRNA. Cultures were untreated (control) or treated with 8-OH-DPAT (40 μM, 5 min) in the absence or presence of α-Me-5HT (20 μM, added 10 min before 8-OH-DPAT treatment). *Enlarged versions* of the *boxed regions* of dendrites are shown beneath each of the images. *G*, quantitative analysis of surface GFP-NR2B clusters (cluster density, size, and intensity) along dendrites under different treatments. *, $p < 0.01$, ANOVA.

any of these drug administrations. Taken together, these results suggest that endogenous serotonin regulates PFC NMDAR surface expression *in vivo* through 5-HT$_{1A}$ and 5-HT$_{2A/C}$ receptors in a counteractive manner.

NR1 and NR2 subunits have to be co-assembled before leaving the endoplasmic reticulum and being transported along microtubules in dendrites to synapses. Our previous study (21) shows that 5-HT$_{1A}$ receptors primarily target NR2B subunit-containing NMDA receptors, consistent with NR2B being the cargo of the microtubule motor KIF17. With the application of fluoxetine plus ketanserin, the surface levels of NR1 and NR2B were reduced to a similar degree (surface NR2A was also reduced, data not shown). It suggests that this reduction likely results from endogenous NR1/ NR2B heteromers and NR1/ NR2A/NR2B triheteromers.

DISCUSSION

It is well known that many antidepressants and antipsychotics exert their actions by inhibiting serotonin reuptake and thus enhance serotonergic transmission (37, 38). Because serotonin has multiple receptor subtypes, systemic elevation of serotonin can induce diverse physiological effects in neurons (2). The molecular mechanisms for serotonin to regulate cellular targets through different subtypes of receptors remain to be identified. We have previously found that 5-HT$_2$ and 5-HT$_4$ receptors are linked to regulate GABA$_A$ receptors (9, 39), whereas 5-HT$_{1A}$ receptors are linked to regulate NMDA receptors in PFC neurons (21). The specific coupling of different 5-HT receptors to distinct ion channels allows serotonin to regulate multiple targets in a precise but flexible manner. Here, we provide evidence showing that the 5-HT$_{1A}$ regulation of NMDARs can be modified by 5-HT$_{2A/C}$ receptor activation, which provides a mechanism to fine-tune the effect of serotonin on NMDAR-mediated synaptic transmission and plasticity.
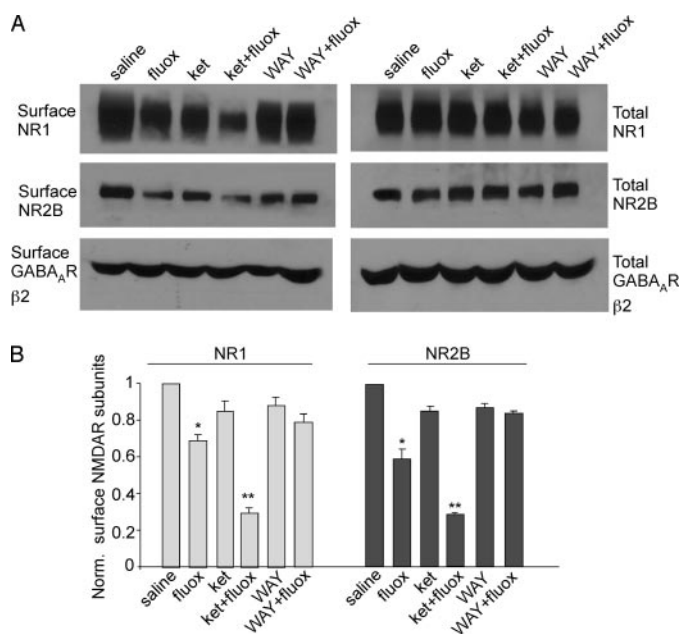
Under normal physiological conditions, which of the one or more 5-HT receptors in PFC pyramidal neurons that are activated by serotonin is determined by the serotonergic projection from dorsal raphe to cellular compartments rich in different subtypes of receptors (40). Agonist binding studies indicate that 5-HT$_1$ and 5-HT$_2$ receptors have different affinities (nanomo-

injected with fluoxetine (20 mg/kg). Surface proteins were labeled with Sulfo-NHS-LC-biotin, and then biotinylated surface proteins were separated from non-labeled intracellular proteins by reaction with NeutrAvidin beads. Surface and total proteins were subjected to electrophoresis and probed with an antibody against the NR1 or NR2B subunit. As shown in Fig. 10 (*A* and *B*), the surface levels of NR1 and NR2B in PFC slices were significantly lower in animals exposed to fluoxetine (NR1: $70 \pm 3\%$ of control; NR2B: $60 \pm 6\%$ of control; $n = 4$). Consistent with electrophysiological results, the fluoxetine-induced reduction of surface NMDARs was more prominent in animals co-injected with the 5-HT$_{2A/C}$ antagonist ketanserin (NR1: $29 \pm 3\%$ of control; NR2B: $30 \pm 1\%$ of control; $n = 4$) and was largely blocked in animals co-injected with the 5-HT$_{1A}$ antagonist WAY-100635 (NR1: $82 \pm 5\%$ of control; NR2B: $84 \pm 1\%$ of control; $n = 4$). The surface GABA$_A$R β_2 subunit level, as well as the total NR1 or NR2B level, in PFC slices was unchanged by

FIGURE 10. **The surface NMDAR level is reduced in PFC from fluox-etine-injected animals.** *A*, Western blot analysis showing the surface and total NR1, NR2B, and GABA$_A$R β2 subunits in lysates of PFC slices taken from animals receiving a single intraperitoneal injection of saline, fluox-etine, ketanserin, ketanserin plus fluoxetine, WAY-100635, or WAY-100635 plus fluoxetine (all drugs are 20 mg/kg). *B*, quantification of sur-face NMDAR subunits in PFC slices from animals treated with different drugs. *, $p < 0.01$; **, $p < 0.001$; ANOVA.

lar *versus* low micromolar) to 5-HT, suggesting that 5-HT$_1$ receptor activation may play a dominant role in response to serotonin. Microdialysis studies have shown that synaptic con-centration of serotonin can reach up to 6 mM (41), suggesting that sometimes all 5-HT receptors could be fully activated at synapses. Both 5-HT$_{1A}$ and 5-HT$_{2A}$ receptors are expressed at dendritic shafts and spines of PFC pyramidal neurons (42, 43), where NMDA receptors are abundant, prompting us to specu-late that both receptors may interact with NMDA receptors in synergistic or opposite ways. Our studies in PFC pyramidal neurons from both acute slices and intact animals treated with various 5-HT-related drugs indicate that blocking 5-HT$_{2A/C}$ receptors unmasks the ability of 5-HT$_{1A}$ receptors to reduce NMDAR currents, suggesting that 5-HT$_{1A}$ and 5-HT$_{2A/C}$ receptors converge on NMDAR channels in a counteractive manner. Similar to serotonin, it has been shown that, in response to dopamine, D$_1$ and D$_2$ receptors that are linked to distinct signaling cascades regulate cortical GABAergic inhibi-tion in an opposing manner (44).

Our previous study has shown that activation of 5-HT$_{1A}$ receptors suppresses NMDAR currents by reducing microtu-bule stability and the ensuing NMDAR trafficking along den-dritic microtubules (21). In this study, we found that activa-tion of 5-HT$_{2A/C}$ receptor opposes the ability of 5-HT$_{1A}$ to induce microtubule depolymerization, suggesting that microtubule dynamics and the microtubule-based NMDAR transport are regulated by 5-HT$_{1A}$ and 5-HT$_{2A/C}$ receptors in a counteractive fashion.

The stability of microtubules is regulated by different micro-tubule-associated proteins (MAPs) in distinct neuronal com-partments. The phosphorylation state of MAP2, a dendrite-

specific MAP, determines the ability of MAP2 to associate and stabilize dendritic microtubules (45). One key signaling mole-cule that regulates MAP2 phosphorylation is ERK (28). Our previous study suggests that 5-HT$_{1A}$ activation suppresses ERK activity, which leads to the decreased MAP2 phosphorylation, MAP2-microtubule interaction, and microtubule stability (21). It is possible that 5-HT$_{1A}$ and 5-HT$_{2A/C}$ oppositely regulates ERK activity, thereby controlling microtubule stability in a counteractive manner. Consistently, our biochemical and immunocytochemical data show that 5-HT$_{2A/C}$ activation potently enhances ERK activity in the dendrites of PFC cultures.

How does the 5-HT$_{2A/C}$ receptor activate ERK? Phospho-lipase C and inositol 1,4,5-trisphosphate, two downstream mol-ecules of classic 5-HT$_2$ signaling, are not involved in this regu-lation (data not shown). Recent studies have suggested that the scaffolding protein β-arrestin, which binds to the third intra-cellular loop of certain G protein-coupled receptors, induces ERK activation (31, 32). 5-HT$_{2A}$ receptors are found to bind purified β-arrestin (46). However, whether 5-HT$_{2A}$ activates mitogen-activated protein kinase via β-arrestin pathway is essentially unknown. Our data show that knockdown of β-ar-restin1/2 not only blocks the 5-HT$_{2A/C}$-induced ERK activation but also eliminates the counteractive effect of 5-HT$_{2A/C}$ on 5-HT$_{1A}$ reduction of NMDAR currents. In addition, we found that the 5-HT$_{2A/C}$ action is dependent on Src activation and clarthin/dynamin-mediated endocytosis of the receptor. Taken together, 5-HT$_{2A}$, via the β-arrestin/Src/dynamin cascade, induces ERK activation to oppose the effect of 5-HT$_{1A}$ on NMDAR functions.

Several mechanisms have been proposed for the regulation of NMDAR functions, including altering the phosphorylation state and biophysical properties of the channel (47, 48) and changing NMDAR trafficking and channel numbers at the membrane (49, 50). Our previous finding suggests that 5-HT$_{1A}$ decreases surface NR2B clusters in a microtubule-dependent manner (21), consistent with the role of cytoskeleton-based transport on NMDAR insertion to the plasma membrane (51, 52). Our immunocytochemical data show that the 5-HT$_{1A}$ reduction of surface NR2B clusters is attenuated by pretreat-ment with a 5-HT$_{2A/C}$ agonist, confirming that 5-HT$_{1A}$ and 5-HT$_{2A/C}$ oppositely regulate NMDAR trafficking. Moreover, 5-HT$_{2A/C}$ opposes the 5-HT$_{1A}$ reduction of surface NR2B clus-ters in a β-arrestin-dependent manner, consistent with the β-arrestin dependence of the 5-HT$_{2A/C}$ action on 5-HT$_{1A}$ regulation of NMDAR currents. Surface biotinylation exper-iments using PFC from intact animals subject to acute fluox-etine treatment have also confirmed the results found in cultured neurons.

Based on the experimental data, we speculate that, in response to serotonin, both 5-HT$_{1A}$ and 5-HT$_{2A/C}$ receptors localized in PFC pyramidal neurons are activated, which converge to regulate NMDAR trafficking and function in an opposite manner, by coupling to distinct signaling cascades and differentially affecting microtubule stability. This study may provide significant insights into the complex regulation of NMDAR-mediated synaptic transmission and plasticity by different serotonin receptors in the PFC network.

REFERENCES

1. Buhot, M. C. (1997) *Curr. Opin. Neurobiol.* **7,** 243–254
2. Andrade, R. (1998) *Ann. N. Y. Acad. Sci.* **861,** 190–203
3. Martin, G. R., Eglen, R. M., Hamblin, M. W., Hoyer, D., and Yocca, F. (1998) *Trends Pharmacol. Sci.* **19,** 2–4
4. Gross, C., Zhuang, X., Stark, K., Ramboz, S., Oosting, R., Kirby, L., Santarelli, L., Beck, S., and Hen, R. (2002) *Nature* **416,** 396–400
5. Saudou, F., Amara, D. A., Dierich, A., LeMeur, M., Ramboz, S., Segu, L., Buhot, M. C., and Hen, R. (1994) *Science* **265,** 1875–1878
6. Heisler, L. K., Chu, H. M., Brennan, T. J., Danao, J. A., Bajwa, P., Parsons, L. H., and Tecott, L. H. (1998) *Proc. Natl. Acad. Sci. U. S. A.* **95,** 15049–15054
7. Goldman-Rakic, P. S. (1995) *Neuron* **14,** 477–485
8. Miller, E. K. (1999) *Neuron* **22,** 15–17
9. Feng, J., Cai, X., Zhao, J., and Yan, Z. (2001) *J. Neurosci.* **21,** 6502–6511
10. Araneda, R., and Andrade, R. (1991) *Neuroscience* **40,** 399–412
11. Penington, N. J., and Kelly, J. S. (1990) *Neuron* **4,** 751–758
12. Aghajanian, G. K., and Marek, G. J. (1999) *Brain Res.* **825,** 161–171
13. Schreiber, R., and De Vry, J. (1993) *Prog. Neuropsychopharmacol. Biol. Psychiatry* **17,** 87–104
14. Burnet, P. W., Eastwood, S. L., and Harrison, P. J. (1996) *Neuropsychopharmacology* **15,** 442–455
15. Tsai, G., and Coyle, J. T. (2002) *Annu. Rev. Pharm. Toxicol.* **42,** 165–179
16. Javitt, D. C., and Zukin, S. R. (1991) *Am. J. Psychiatry* **148,** 1301–1308
17. Jentsch, J. D., and Roth, R. H. (1999) *Neuropsychopharmacology* **20,** 201–225
18. Mohn, A. R., Gainetdinov, R. R., Caron, M. G., and Koller, B. H. (1999) *Cell* **98,** 427–436
19. Law, A. J., and Deakin, J. F. (2001) *Neuroreport* **12,** 2971–2974
20. Boyer, P. A., Skolnick, P., and Fossom, L. H. (1998) *J. Mol. Neurosci.* **10,** 219–233
21. Yuen, E. Y., Jiang, Q., Chen, P., Gu, Z., Feng, J., and Yan, Z. (2005) *J. Neurosci.* **25,** 5488–5501
22. Yuen, E. Y., Jiang, Q., Feng, J., and Yan, Z. (2005) *J. Biol. Chem.* **280,** 29420–29427
23. Wang, X., Zhong, P., Gu, Z., and Yan, Z. (2003) *J. Neurosci.* **23,** 9852–9861
24. Jiang, Q., Yan, Z., and Feng, J. (2006) *J. Neurosci.* **26,** 4318–4328
25. Luo, J. H., Fu, Z. Y., Losi, G., Kim, B. G., Prybylowski, K., Vissel, B., and Vicini, S. (2002) *Neuropharmacology* **42,** 306–318
26. Arvanov, V. L., Liang, X., Russo, A., and Wang, R. Y. (1999) *Eur. J. Neurosci.* **11,** 3064–3072
27. Ray, L. B., and Sturgill, T. W. (1987) *Proc. Natl. Acad. Sci. U. S. A.* **84,** 1502–1506
28. Sanchez, C., Diaz-Nido, J., and Avila, J. (2000) *Prog. Neurobiol.* **61,** 133–168
29. Payne, D. M., Rossomando, A. J., Martino, P., Erickson, A. K., Her, J. H., Shabanowitz, J., Hunt, D. F., Weber, M. J., and Sturgill, T. W. (1991) *EMBO J.* **10,** 885–892
30. Mao, L., Tang, Q., Samdani, S., Liu, Z., and Wang, J. Q. (2004) *Eur. J. Neurosci.* **19,** 1207–1216
31. Luttrell, L. M., Ferguson, S. S., Daaka, Y., Miller, W. E., Maudsley, S., Della Rocca, G. J., Lin, F., Kawakatsu, H., Owada, K., Luttrell, D. K., Caron, M. G., and Lefkowitz, R. J. (1999) *Science* **283,** 655–661
32. Lefkowitz, R. J., and Shenoy, S. K. (2005) *Science* **308,** 512–517
33. Attramadal, H., Arriza, J. L., Aoki, C., Dawson, T. M., Codina, J., Kwatra, M. M., Snyder, S. H., Caron, M. G., and Lefkowitz, R. J. (1992) *J. Biol. Chem.* **267,** 17882–17890
34. Sever, S. (2002) *Curr. Opin. Cell Biol.* **14,** 463–467
35. Gout, I., Dhand, R., Hiles, I. D., Fry, M. J., Panayotou, G., Das, P., Truong, O., Totty, N. F., Hsuan, J., and Booker, G. W., *et al.* (1993) *Cell* **75,** 25–36
36. Ahn, S., Maudsley, S., Luttrell, L. M., Lefkowitz, R. J., and Daaka, Y. (1999) *J. Biol. Chem.* **274,** 1185–1188
37. Deakin, J. F. (1988) *Pharmacol. Biochem. Behav.* **29,** 819–820
38. Artigas, F., Romero, L., de Montigny, C., and Blier, P. (1996) *Trends Neurosci.* **19,** 378–383
39. Cai, X., Flores-Hernandez, J., Feng, J., and Yan, Z. (2002) *J. Physiol.* **540,** 743–759
40. Amargos-Bosch, M., Bortolozzi, A., Puig, M. V., Serrats, J., Adell, A., Celada, P., Toth, M., Mengod, G., and Artigas, F. (2004) *Cereb. Cortex* **14,** 281–299
41. Bunin, M. A., and Wightman, R. M. (1999) *Trends Neurosci.* **22,** 377–382
42. Kia, H. K., Brisorgueil, M. J., Hamon, M., Calas, A., and Verge, D. (1996) *J. Neurosci. Res.* **46,** 697–708
43. Jakab, R. L., and Goldman-Rakic, P. S. (1998) *Proc. Natl. Acad. Sci. U. S. A.* **95,** 735–740
44. Trantham-Davidson, H., Neely, L. C., Lavin, A., and Seamans, J. K. (2004) *J. Neurosci.* **24,** 10652–10659
45. Brugg, B., and Matus, A. (1991) *J. Cell Biol.* **114,** 735–743
46. Gelber, E. I., Kroeze, W. K., Willins, D. L., Gray, J. A., Sinar, C. A., Hyde, E. G., Gurevich, V., Benovic, J., and Roth, B. L. (1999) *J. Neurochem.* **72,** 2206–2214
47. Lieberman, D. N., and Mody, I. (1994) *Nature* **369,** 235–239
48. Wang, Y. T., and Salter, M. W. (1994) *Nature* **369,** 233–235
49. Vissel, B., Krupp, J. J., Heinemann, S. F., and Westbrook, G. L. (2001) *Nat. Neurosci.* **4,** 587–596
50. Wenthold, R. J., Prybylowski, K., Standley, S., Sans, N., and Petralia, R. S. (2003) *Annu. Rev. Pharmacol. Toxicol.* **43,** 335–358
51. Setou, M., Nakagawa, T., Seog, D. H., and Hirokawa, N. (2000) *Science* **288,** 1796–1802
52. Guillaud, L., Setou, M., and Hirokawa, N. (2003) *J. Neurosci.* **23,** 131–140
53. Schwarze, S. R., Ho, A., Vocero-Akbani, A., and Dowdy, S. F. (1999) *Science* **285,** 1569–1572